The Development and Testing of Low-Cost Heat Transfer Enhancements for Solar Dryers

Hoda Mahmoodi

Thesis for the degree of Master of Science in Engineering
Division of Energy and Building Design
Department of Energy Sciences
Faculty of Engineering | Lund University

The Development and Testing of Low-Cost Heat Transfer Enhancements for Solar Dryers

Hoda Mahmoodi

June 2023, Lund

This degree project for the degree of Master of Science in Engineering has been conducted at the Division of Energy and Building Design, Department of Energy Sciences, Faculty of Engineering, Lund University.

Supervisor at the Division of Energy and Building Design was Dr Henrik Davidsson.
Supervisor at Bhutan University was Samten Lhendup.

Co- Supervisor at Lund University was Himani Garg.

Examiner at Lund University was Dr Martin Andersson.

The project was carried out in cooperation between Lund University and the Royal University of Bhutan and was funded by the Swedish Research Council.

Thesis for the Degree of Master of Science in Engineering

ISRN LUTMDN/TMHP-23/5546-SE

ISSN 0282-1990

Department of Energy Sciences

Faculty of Engineering, Lund University

Sweden

www.energy.lth.se

Abstract

In the mountainous regions of Bhutan and Nepal, post-harvest losses cause significant challenges for producers. Open air sun drying is usually used by farmers to preserve their produce. There are many disadvantages to this method. The Swedish Research Council is supporting a project called Solar Food: Reducing Post-Harvest Losses Through Improved Solar Drying, which aims to create a low-cost solar-powered food dryer to enhance the quality of food preservation in the Himalayas region.

In this project, the thermal characteristics of various components of a solar dryer were analyzed at different air flows, including the heat exchanger, absorber, and drying chamber. The data is used to compute efficiency and heat fluxes, and drying rates are assessed to establish the optimum flow. The effect of adding a net as artificial roughness to the absorber was also examined to identify potential areas for improvement in thermal performance.

The results indicate that increasing airflow reduces drying times, as higher flows facilitate faster moisture removal, resulting in shorter drying durations, Additionally, the study revealed a homogeneous drying process within the chamber, indicating that the samples dried uniformly. The study also demonstrated an inverse relationship between higher flow rates and lower heat exchanger efficiencies. Based on the results of the experiment evaluating the effectiveness of a chamber with holes in its walls, the chamber without holes performed slightly better than the chamber with holes. However, product thickness, sunlight, and wind may have impacted the measurements.

In terms of absorber efficiency, the study reveals that flow has minimal impact within this project's scope. Nonetheless, it is inconclusive to compare the efficiency of solar dryer with and without a net on the absorber based on these tests because of the varying weather conditions.

For a more accurate assessment of the impact of nets on absorber efficiency in the future, it is recommended to conduct experiments in a controlled environment. Furthermore, exploring the use of nets with various orientations on the surface of the absorber may reveal opportunities for enhancing heat transfer.

Acknowledgments

I would like to express my sincerest gratitude and appreciation to everyone who has helped me throughout this master's thesis journey.

First and foremost, I would like to express my deepest gratitude to my supervisor, Dr. Henrik Davidsson, for all the support, guidance, and continuous encouragement. I am truly grateful for your dedication, patience, and mentorship throughout the process. Your insightful comments, constructive criticism, and humorous asides made my work much more enjoyable.

I would like to express my special gratitude to my supervisor in Bhutan, Samten Lhendup, for your constant support and friendship.

I would like to thank Dr. Tshewang Lhendup for their kindness, hospitality, and generosity during my stay in Bhutan. Their warm welcome made my time there truly unforgettable.

Furthermore, I am grateful for the help from my examiner, Dr. Martin Andersson, during my dissertation's preparation and completion.

My heartfelt gratitude goes to my family and friends for their emotional support, encouragement, and motivation along this journey. Their belief in me and confidence in my talents have been a steady source of inspiration during this challenging journey.

Finally, I would like to express my sincere gratitude to all those who have contributed to this thesis and my overall academic journey and gave their time and shared their experiences with me, without whom this research would not have been possible.

Thank you all for your invaluable contributions to this thesis.

Table of Contents

1. Introduction

1.1. Project introduction

The primary method of preserving food by man was most likely drying (Alamu, et al., 2010). In this process, moisture is removed from agricultural produce to provide a product that can be stored safely for an extended period. When food reaches 63 °C, microorganisms are effectively killed. Foods that are dried do not require any special equipment for storage or transportation (Waewsak, et al., 2006). Traditional open-air sun-drying methods of dehydrating vegetables and other food crops are unsatisfactory because they deteriorate rapidly. Agricultural produce dried with solar dryers has been shown to be more flavorful, colorful, and mold-free than sun-dried agricultural produce. (Gallali, et al., 2000). Using dryers in developing countries can reduce post-harvest losses and increase food availability. These losses are generally estimated to be 40 %, but they can be nearly as high as 80 %, under very adverse conditions. An estimated significant share of these losses is caused by improper and/or untimely drying cereal grains, pulses, tubers, meat, fish, Etc. (Togrul and Pehlivan, 2004). Because it is the most simple and cheapest method of conserving foodstuffs, traditional drying is widely used in developing countries. It is frequently done on the ground in the open air. Several problems can arise when drying food in the open, such as getting wet or dusty, drying too quickly or too slowly, exposing the food to direct sunlight, pest infestation, animal attacks, etc. (Madhlopa, et al., 2002). A longer lifespan of food allows for longer transport, which is beneficial in e.g., mountainous areas where small roads meander between the mountains making it much less accessible for large-scale transport. Solar dryers have been suggested to reduce post-harvest losses in Himalayan regions. The process of food drying has been used widely in Bhutan for its low cost and accessibility to farmers; however, direct sunlight can cause nutrient degradation that can degrade the quality of the finished product (Henrik Davidsson., 2017). The Bhutanese population is currently suffering from nutrient deficiency. By improving food preservation methods, spoilage can be reduced, and nutrient degradation minimized (WFP 2020).

Profitability should increase by reducing food waste and improving the situation for farmers. Therefore, it will be necessary to improve the design and thermodynamics of the solar dryer to achieve higher drying rates and shorter drying times.

1.2. Aim and research questions

The master's thesis is part of the Solar Food project: Reducing post-harvest losses through improved solar drying. This project aims to improve farmers' livelihoods, contribute to rural development, and ensure local food security by developing a locally adapted solar dryer for crop drying. In collaboration with the Royal University of Bhutan, Lund University made this project possible.

This thesis seeks to increase heat transfer by focusing on disrupting the flow in the absorber of a solar dryer with different net arrangements. A high production rate can be attained through efficient heat transfer because it accelerates the drying of products.

The eggplant was selected as the sample for evaluation in this project and the solar dryer was evaluated by measuring the temperatures of the dryer before and after adding a net to the absorber. Based on the collected data, a performance analysis was conducted on each component under different flow rates to understand the dryer and its limitations better.

To conduct the experiments, the following questions were considered:

- Question 1: What ways to disturb the flow, and how does it affect heat transfer and losses?
- Question 2: How does the airflow temperature in the drying chamber affect the drying rate?

2. Background

2.1. Bhutan

Bhutan, a landlocked country in the Eastern Himalayas, is one of the world's ten global biodiversity hot spots. It has a total land area of around 47 000 km² (World Bank, 2005). Almost the entire country is mountainous, with an elevation ranging from 100 m above sea level in the south to over 7500 m in the north. In Bhutan, three major landforms can be observed: steep hills and dense forests in the southern foothills, broad river valleys in the inner Himalayas, and snow-covered peaks in the high Himalayas. Furthermore, Bhutan's climate varies according to its three landforms. There is a high level of humidity in the southern foothills of the Himalayas, while a cool, temperate climate prevails in the inner Himalayas with an annual rainfall of 1000 mm, and a severe alpine climate dominates in the high Himalayas with a rainfall of only 400 mm (Climate Research Unit of University of East Anglia, 2020).

2.1.1. Bhutan's Economic and Social Setting

Most of the population lives in the valleys of the nation, at an altitude of 1000-3000 m. Bhutan began modernizing its economy in the early 1960s by establishing basic infrastructure such as roads, electricity, telecommunications, and transportation (Whalley, 2004). Since 1981, Bhutan's economy has developed robustly, transitioning from a non-monetized agriculture-based traditional economy to a modern wage-based exchange economy (Frame, 2005). The Bhutanese economy remains largely dependent on agriculture. According to the United Nations, approximately 79 % of the world's population depends on agriculture for their livelihood. It contributed about 33 % of the country's GDP in 2002 (16.2 % from agriculture, 7 % from livestock, and 9.8 % from forestry). In addition to being physically difficult, the mountainous topography also creates a more sensitive climate. As a result of the rapid climate change that is occurring today and, in the future, Bhutan's agriculture is likely to be adversely affected (Chhogyel and Kumar, 2018). Because of these developing challenges, a better food preservation system must be developed. Reducing post-harvest losses would enhance yields, which might help buffer the looming losses caused by a harsher environment.

2.2. Solar drying technology

Numerous varieties of solar dryers have been developed recently to reduce post-harvest losses and raise the caliber of agricultural output. Solar drying confirms perfect drying and the required quality of the finished product under controlled temperature and moisture removal rates. However, very few solar dryer designs are used commercially or on larger scales than demo projects (Sharma et al., Udomkun et al., 2020). Solar dryers are classified according to their size, design, and method of solar energy consumption for agricultural and marine products.

2.2.1. Direct passive solar dryers

Direct passive Solar dryers with natural convection are simple and affordable to build. In passive solar dryers, the drying chamber is typically made up of a transparent sheet of glass, polyethylene, or polycarbonate that is thermally insulated (Hamdi et al., 2018; Jain et al., 2004). Through pressure gradients, buoyancy forces, or a combination of both, the air heated by solar radiation is forced to pass over the crops (Tomar et al., 2017).

While the product is drying, some solar radiation transfers to the cabinet and is absorbed by the drying product, while the ambient light reflects the remainder. Depending on the material being dried, the airflow rate, and the location, the typical drying effectiveness of a passive solar dryer can be anywhere from 20 % to 40 % (Kumar et al., 2016). The ratio of the energy used to heat the sample from moisture evaporation to the total energy consumed is known as the dryer's efficiency**.**

2.2.2. Indirect passive solar dryer

A solar air collector and a drying chamber are the components of an indirect passive solar dryer that uses forced convection. A low-pressure solar air collector warms the air before it enters the drying chamber and flows over the

drying tray in an air duct. The moist air is released from the drying chamber through air vents or a chimney at the top (Tiwari, 2016; El-Sebaii et al., 2012). Indirect passive solar dryers typically have a drying efficiency between 13 and 25 %, which is lower than that of direct solar dryers (Kumar et al., 2016). Passive dryers are recommended to be used for drying fruits and vegetables in small batches.

2.2.3. Active Solar Dryers

An active solar dryer uses an air circulation system to circulate the heated air within the drying unit or from the solar air heater to the drying unit. The air is circulated in the drying chamber by an external arrangement. Electric fans or blowers run on electricity generated by photovoltaic panels or grids and circulate the air for drying. An exhaust fan moves the air, and these solar dryers can be used for extensive commercial drying operations. Compared to passive solar dryers, these dryers have been developed to be more suitable for drying crops with high moisture content, such as kiwi, papaya, cabbage, and cauliflower (Ghatrehsamani et al., 2012; Bala and Woods, 1994). A dryer with an active drive requires more capital investment, and its operating and maintenance costs are also higher to achieve high product quality and drying efficiency (Mujumdar, 2006).

2.3. The food dryer

This project's dryer is made up of a heat exchanger, an absorber, heat storage, a drying chamber with seven shelves, an interior fan, and an external fan. The product is located on shelves inside the drying chamber. Thus, the crop is not directly exposed to solar radiation. First, the air is heated as it travels across an absorber after entering a circular inlet and passing over a flat piece of the aluminum sheet used as a heat exchanger. The heated air then travels through the heat storage and into the drying chamber, where it is combined with colder, more humid air recirculated from the internal fan. The air then travels

down the heat exchanger's opposite side before being released into the surrounding environment through the vent.

The dryer is illustrated in Figure 1, where the numbers 1 and 9 correspond to the dryer's inlet and outlet, respectively.

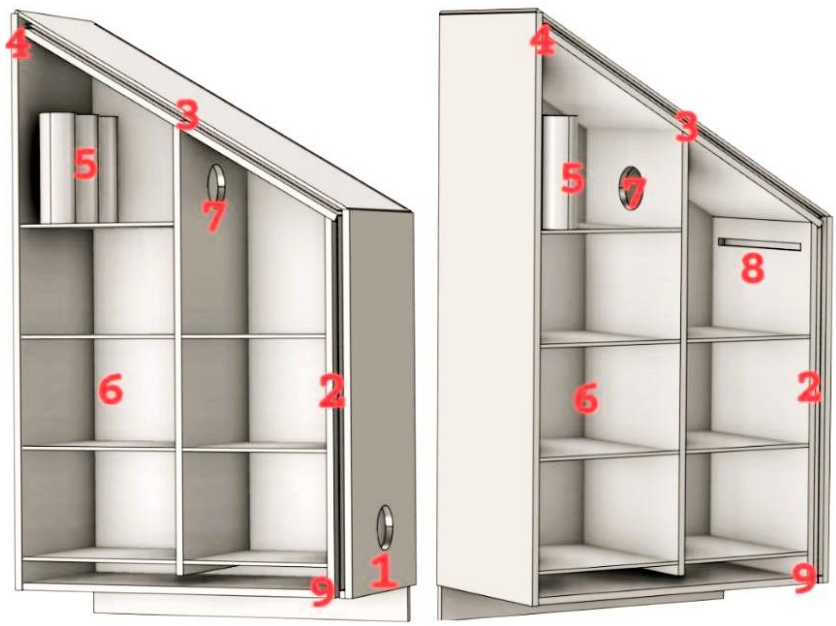

Figure 1. The food dryer's 3D model is viewed from two distinct angles. According to the picture, the numbered pieces include the following, which are arranged in sequential sequence based on the air flow through the dryer. 1. Dryer inlet; 2. Heat exchanger; 3. Absorber; 4. Absorber outlet; 5. Heat storage; 6. Drying chamber; 7. Internal fan; 8. Drying chamber outlet; 9. Dryer outlet.

2.4. Heat transfer and losses

An understanding of heat transfer is crucial in furthering the design because the efficiency of a solar dryer ultimately depends on energy balances. Heat transfer begins when a temperature is differential within a medium or between media. This process is characterized by the three modes of energy transfer conduction, convection, and radiation. Transfer of energy from one thing to another, or between objects in touch, due to a temperature difference, is called conduction, and it happens in solids and stationary fluids. Convection transfers heat from one body to another through fluid movement in contact with a surface of a different temperature. While buoyancy forces drive fluid motion in natural convection, fans, and pumps are typically used to generate flow in forced convection. When a surface emits energy in the form of electromagnetic waves, it can transfer heat to the surrounding space via a process known as radiation (Bergman et al., 2011).

2.4.1. Conductivity

During conduction, interactions between particles with different energies transfer energy from more energetic to less energetic molecules. Conduction through a medium is determined by the geometry and material of the medium, as well as its ability to conduct heat and transient changes in its properties. Dryer heat is transferred through the wooden walls and insulation, separating the exterior and interior spaces. Heat transfer through a wall is proportional to the difference in temperatures on either side. The following equation describes this heat flux (Engineering ToolBox, 2003):

$$q = A(\frac{k}{s})\Delta T \qquad Eq.1$$

Where k represents the conductivity constant of the material, s represents the wall thickness, and ΔT is the temperature gradient across the wall. Therefore, several layers of insulation adhered to the exterior of the dryer used in this project to minimize thermal conductivity losses.

2.4.2. Convection

Although convective heat transfer is essential when redesigning the solar dryer, radiative heat transfer is still at the heart of the absorber. These forces predominate in the heat exchanger and are responsible for the heat losses through the solar dryer's walls. Eq. 2 describes the convective forces between two mediums (Engineering ToolBox 2003):

$$Q = h_c \cdot A \cdot \Delta T \qquad Eq.2$$

A represents the surface area where the heat transfer occurs, Q denotes the convective heat transfer, h_c denotes the convective constant of the system, and ΔT denotes the temperature difference between the surface in contact with the fluid and the average temperature of the fluid.

2.4.3. Radiative

The term radiative heat transfer refers to the release of thermal energy in the form of electromagnetic radiation by any mass above absolute zero Celsius. Radiated waves have a wavelength that varies with the object's temperature but is typically in the infrared range for practical purposes (Engineering Toolbox, 2003). A body's rate of radiating energy can be calculated using the following equation:

$$Q = \varepsilon \sigma T^4 A \qquad Eq.3$$

The second is the surface's emissivity, which is represented by ε in Eq. 3 and indicates that some surfaces are more effective at radiating energy than others. Black bodies are defined as bodies with maximum emissivity. They have an emissivity of 1. An emissivity value closer to zero indicates that the surface is a poor emitter. Stefan-constant Boltzmann's represented by σ in Eq. 3 is approximately $5.67 \cdot 10^8$ $\mathrm{W/(m^2K^4)}$.

The JNEC university in Bhutan has installed a glass layer above the absorber on the dryer to capture some of the radiation the absorber emits. The radiation losses of the system are decreased because some of the radiation is reflected or re-emitted by the glass. But it will also cut down on the sunlight reaching the absorber. Therefore, unless the radiative thermal losses are significant,

adding more glass layers to a system could have an adverse effect (Davidsson, 2021).

2.5. Heat flux and Density of Air

Multiplying the mass flow F_m, the specific heat of air C_p and the temperature change over a second ΔT yields the heat flux, which is the heat energy transmitted per second for a given airflow. Following is an equation that can be used to determine heat flux:

$$Q = F_m C_p \Delta T \qquad Eq.4$$

The volumetric flow rate can be calculated by multiplying the average inflow velocity by the cross-sectional area of the inlet and then by the air density.

$$F_m = V_{air} A_{cross} \rho_{air} \qquad Eq.5$$

Combining Eq. 4 and Eq. 5 leads to the following equation for the flux:

$$Q = V_{air} A_{cross} \rho_{air} C_p \Delta T \qquad Eq.6$$

During the appropriate temperature range, air's isobaric specific heat is approximately $1.01\ \mathrm{kJ/(kg \cdot K)}$ (Engineering Toolbox ,2004). The density of air at 1 atmosphere and 25 °C is around $1.17\ \mathrm{kg/m^3}$. (Engineering Toolbox, 2003). The dryer was located at an altitude of roughly 900 m above sea level, and the air density and pressure were different from those at sea level (JNEC u.d, 2022). Finding the air pressure at 900 m above sea level is the first step in determining the density of the air (Engineering Toolbox, 2003):

$$p = p_{atm}(1 - 2.25577\ .\ 10^{-5} h)^{5.25588} \qquad Eq.7$$

Assume that h is the height in meters, and that P_{atm} is 1 atmosphere. As a result, the atmospheric pressure is 0.91 mbar higher up at an altitude of 900 meters. Density is then determined by applying the ideal gas law:

$$PV = RT \qquad Eq.8$$

Volume can be rewritten as weight divided by density to find the density solution:

$$\rho = \frac{Pm}{RT} \qquad Eq.9$$

Dividing both sides with the same equation but for the standard density and pressure found at sea level with the same mass and temperature, this equation can be achieved:

$$\frac{\rho}{\rho_{atm}} = \frac{P}{P_{atm}} \qquad Eq.10$$

It can be determined that the density of air at 900 m altitude is approximately $1.05\ \mathrm{kg/m^3}$, which can be used in the heat flux equation to ensure that energy and efficiency calculations are accurate.

2.6. Heat exchanger

Heat exchangers are devices that aim to increase heat transfer between two bodies. This case involves two air streams, the outlet and inlet air. A heat exchanger could be incorporated to use the excess heat to pre-heat the incoming air before it reaches the absorber. This would result in reduced heat losses, greater thermal efficiencies, and higher drying temperatures since the thermal energy would be repurposed within the dryer. The following equation can be used to determine the efficiency of a heat exchanger under the assumption that the mass flow on both side is equal (Çengel and Ghajar., 2002):

$$\eta = \frac{T_{out\_c} - T_{in\_c}}{T_{in\_h} - T_{in\_c}} \qquad Eq.11$$

Efficiency can be calculated as the ratio of the difference across one side, in this case, the cold side, to the difference between the inlets on both sides. A complete temperature transition between the two sides is needed to achieve 100 % efficiency. In other words, the hot side's intake and the cold side's output are at the same temperature.

Leakage problems can be detected with the help of the heat exchange. Without any air leaks, the principle of conservation of mass requires that airflow will be identical on both sides of the heat exchanger. Due to the principle of energy conservation, the temperature differential on either side of the heat exchanger should be the same because the heat capacity of air varies very little under the relatively minor temperature shift observed in the system. Thus, a continuous comparison between the two parties provides the system with valuable transparency.

2.7. Conception of artificial roughness

Artificial roughness refers to deliberately modifying the absorber's surface in a solar dryer to generate irregularities or rough elements. These irregularities in the absorber's surface cause the air to become turbulent, increasing the heat and mass transfer rate. By increasing convective heat transfer and promoting better air mixing, artificial roughness can boost the efficiency of a solar dryer. The airflow becomes more turbulent as it encounters obstacles and irregularities on a rough surface. The increased interaction between the air and the absorber surface enhances heat transfer and moisture evaporation. Roughness elements can be implemented in several ways, including ribs, wires, protrusions, or textured surfaces. Their size, shape, arrangement, and orientation can be optimized to achieve the desired level of disruption and turbulence in the flow Alam and Kim proposed that roughness parameters such as ribs arrangement, the shape of wires, rib pitch, and rib height affect the heat transfer and friction factor. Various rib arrangements have been investigated, and some arrangements are transverse ribs, angled ribs, V-ribs, W-ribs, multi-V-ribs, ribs with grooves, staggered ribs, chamfered ribs, and discrete ribs. Wang and Sundén conducted an experimental investigation of local heat transfer in a square duct with variously shaped ribs, and they concluded that the local heat transfer in the area is highly dependent on the rib shape.

2.7.1. Methodology of artificial roughness

Laminar flow is dominant over a heated surface due to viscous forces, which exist beneath the turbulent flow core. Poor heat transmission rates from the heated surface to the surrounding air can be attributed to the presence of this viscous sublayer. When artificial roughness is applied to a heated surface, local wall turbulence is induced due to flow dissociation and reattachment between sequential roughness elements. By generating turbulence, roughness features dramatically boost heat extraction rates from heated surfaces. An essential factor in this turbulence is the height of the roughness components. If the roughened surface height exceeds the laminar sublayer thickness, then the roughened surface causes more turbulence, increasing fluid friction and pumping more power. When determining whether artificial roughness promotes a higher heat transfer rate while minimizing friction losses, it is preferable to create turbulence only near the heat transfer surface, i.e., near the viscous sublayer.

According to one report, the ideal value of the relative roughness pitch p/e is 10 (Prasad and Saini, 1988). The ratio between the distance of two consecutive ribs and the height of the rib is known as the relative roughness pitch p/e . For rectangular ducts, the researchers report an optimum rib angle between 45 and 60 degrees,

Based on these details, to conduct this experiment, 100 square ribs with the height of 1 mm would have been required. Unfortunately, the equipment to glue those ribs to the absorber was unavailable in Bhutan. Instead, a net with a distance of 13 mm and a thickness of 1 mm was used.

2.8. Concept of drying process

Removing and releasing moisture from a product into the atmosphere is known as drying or dehydration. Drying is defined as the removal of moisture through the simultaneous transmission of heat and mass. (Brooker et al., 1992; Akpinar and Yaldiz, 2003; Ertekin and Yaldiz, 2004). Two different things happen at once when a solid is heated to dry it:

A. Evaporation of surface moisture through the transfer of energy (mainly as heat) from the surrounding environment.

B. Moisture inside moves to the surface of the object and disappears through evaporation due to the addition of energy.

The speed at which the two processes move can control how quickly things dry. Convection, conduction, radiation, and in some situations, a combination of these phenomena can all result in heat transfer from the surrounding environment to the wet solid (Hale et al., 1971; Bechoff et al., 2009; Chen et al., 2005). Factors such as temperature, air humidity and flow, exposed surface area, and pressure influence Process A, the evaporation of water from a material's surface. The physical properties of the solid, the rate of diffusion, and the moisture content all influence Process B, the transport of moisture within the solid.

In addition to weather, the following factors affect how agricultural crops dry throughout the drying process:

- Product
- Size and shape
- Initial and final moisture content
- Bulk density
- Thickness of the layer
- Temperature, humidity of air in contact with product

2.9. Drying Rate and Surface Area

The drying process usually consists of three main phases. During the initial phase, the product is heated. In the next stage, the moisture evaporates at a constant rate since there are no internal or external mass transfer resistances. External heat transfer is the only means of controlling the drying at this stage. The falling rate is characterized by a slowdown in the drying rate in the third stage. It is caused by the tightly bound water remaining in the product. Two falling rates can sometimes be observed, and it is hypothesized that internal and external mass transfer rates control the first falling rate stage. Based on the hypothesis, the second falling rate only depends on internal mass transfer resistance. Nutriments' drying behaviour correlates with the product’s

porosity, homogeneity, and tendency to absorb moisture from the surrounding air (Rahman and Perera, 2007).

Drying rate, defined here as the amount of water lost to evaporation per unit of area per hour, is a crucial metric throughout this report.

$$Drying\ Rate = \frac{\Delta m}{t_{drying} \cdot A} \qquad Eq.12$$

To ascertain the density of the eggplant, a circular piece of eggplant was cut and its diameter D, height h was measured by a ruler, then calculate the volume of the slice by using the Eq. 13:

$$V = \pi \left(\frac{D}{2}\right)^2 \cdot h \qquad Eq.13$$

The mass of the round portion was measured using a kitchen scale and recorded; the density was then computed.

$$\rho = \frac{m}{V} \qquad Eq.14$$

According to Eq. 14 eggplant has a density of 520 kg/m^3, which can be used to compute the volume of used eggplant given its weight.

2.10. Factors affecting the drying rate

Many parameters, such as drying temperature, relative humidity, air velocity, product starting moisture content, product drying constant, and solid qualities, including density, permeability, and porosity, can affect drying processes. Understanding temperature and moisture movement in the product will aid in enhancing drying methods and food quality as the drying process evolves from basic constant drying settings to sophisticated, time-varying drying schemes (Chua et al., 2002; Panchariya et al., 2002).

2.10.1. Drying temperature

One of the significant factors affecting the drying time is the air temperature used in the process. Since removing water requires a phase transition from liquid to vapor, boosting the dryer's energy input by heating the air will expedite drying. However, ensuring the temperature does not become too high and ruin the product is essential (Mercer., 2014). According to Doymaz (2005), drying times can be reduced by increasing the air temperature in the solar dryer.

2.10.2. Effect of layer thickness

The drying rate is proportional to the amount of water that must travel from the material's interior to the exterior during the drying process. Because of this, drying times for large portions of food are typically longer than those for smaller portions of the same item. The layer shouldn't be too thick to block the hot air from penetrating, but it also shouldn't be too thin to make good use of the available thermal energy. Sarker (2012) conducted tests to determine the optimal drying conditions for potato slices of several thicknesses 3 mm, 5 mm and 7 mm and temperatures 40 °C, 45 °C and 60 °C. Drying time was shown to increase with layer thickness, suggesting that faster drying occurred for thinner layers. 5 mm thickness was considered for the eggplant layer in this research.

2.10.3. Effect of air velocity

For drying to take place efficiently in a solar dryer, sufficient air movement is required. This necessitates the use of a suitable fan, one capable of overcoming the static pressure generated in the drying cabinet and ensuring airflow at the appropriate velocity. According to Murthy (2009), a dryer's performance can be optimized with the right amount of air flow. The temperature of the drying air may rise with a slower air flow rate, while the amount of moisture removed may fall with a faster air flow rate. In this work, the drying rate was measured at three different flow rate of 11 l/s, 15 l/s and 19 l/s.

2.10.4. Water activity

Water activity is a reliable indicator of food preservation and safety by eliminating microorganism growth, physical and chemical reactions, and spoilage of dry food products. The amount of water available to microorganisms in a product is measured on a scale from 0 to 1, with 1 being the highest value. Yeasts and molds require a lower water activity than bacteria. It is estimated that fresh fruits and vegetables have a water activity of between 0.95 and 0.99, while dried nutrients range from 0.6 to 0.85 (Rosengren, 2017).

3. Method

3.1. Preparation and calibration

As a first step, thermocouples were connected to a Campbell Scientific Multiplex 16/32 connected to a Campbell Scientific CR1000 Data Logger. This was done before departing for Bhutan. The data logger was left on overnight in a 25 °C room to ensure accurate readings. In order to ensure that the thermocouples remained accurate at higher temperatures, another test was performed by submerging them in boiling water for a few minutes. In addition to testing thermocouples under warmer conditions, ice water was later used to test them. Before the installation of thermocouples in the dryer, this process was repeated with all thermocouples used in Bhutan.

The dryer was inspected in Bhutan for flaws, such as unnecessary pressure drops and potential leaks. The external and internal fans were installed after the dryer had been up to standard and had all the predetermined features, and the glass cover for the absorber was glued and sealed to the dryer.

To measure solar irradiance and heat flux, a pyranometer with a sensitivity of 9.98 $\mu V/W/m^2$ was placed on the absorber's surface. The pyranometer was attached to the absorber plate's frame to ensure that it had the same orientation as the dryer.

At the locations indicated in Figure 1, twenty-four thermocouples were measured, cut, and labeled before being attached to the dryer. Three thermocouples were installed in each section: one in the middle, one near the left wall (where the door is located), and one opposite the right wall. For the chamber, six thermocouples were arranged in pairs: one pair at the beginning, one pair in the middle, and one pair at the outlet.

Figure 2. There is a thermocouple with a soldered tip placed in the solar dryer chamber.

It was ensured that all thermocouples were adequately prepared to avoid inaccurate readings. At the very tip, a small amount of solder was used to connect the wires after removing 4 mm -5 mm of insulation from the ends. A thermocouple was attached to the dryer deliberately to avoid direct contact

with any surface or direct exposure to thermal radiation from the absorber or the sun. Thus, the circulating air in the dryer was the only direct source of heat in direct contact with the sensor end.

It is vital that the datalogger be connected to the ground to function correctly.

A pipe with a diameter of 154 mm was attached to the dryer's intake to collect data on the air velocity. To get an accurate reading of the pipe input's temperature, protection from direct sunlight was required. These pipes are not part of the final design; rather, they are used to quantify the volume of air entering the dryer.

3.2. Flow Measurements

The flow was determined with the assistance of a standardized method that was detailed in the book "Metoder för mätning av luftflöden i ventilationsinstallationer" (Johansson and Svensson, 1999). When using this technique, the pipe must be at least two times the pipe's diameter away from the fan and at least five times its diameter away from the air inlet. This report was compiled using an infrastructure that far exceeded these criteria. Two holes were drilled into the pipe, one from above and one from the side, to determine the flow. Two perpendicular holes were drilled to accommodate to hot wire anemometer; for each hole, the anemometer was placed 45 mm and 109 mm into the pipe. The average of the four readings was used to determine the wind speed. A pipe has a gradient of air speeds because the air closer to the canter moves faster than the air closer to the wall. For a pipe with a diameter of 154 mm, this point can be found at the depths previously described, where the airspeed equals the average speed of the pipe in this gradient (Johansson and Svensson 1999). In order to calculate the volumetric flow rate, the average air speed at these four points was combined with the pipe's cross-sectional area.

3.3. Eggplant preparation

Fresh eggplant was used for each experiment and was carved into circular shapes with a thickness of 5 mm using a kitchen knife and cutting board. To avoid overlapping, the eggplants were carefully arranged on drying trays. After the required drying time had elapsed, the dried eggplant pieces were taken out of the dryer and weighed using a kitchen scale.

Figure 3. The left image shows two kilograms of eggplants sliced thinly and homogeneously. The slices were then arranged and deposited in every tray of the solar dryer. The right image displays a single tray of sliced eggplants.

3.4. Data Collection and Drying

During the experiment, the internal fan, data logger, and external fan were turned on through a voltage regulator at 10:00 in the morning. It was necessary to adjust the voltage for the external fan to achieve the desired flow, and the flow was tested according to the method described earlier. The voltage was changed if the flow was not at the predetermined level. Setting the voltage and testing the flow were repeated until the desired flow was

achieved. At the end of each day of the experiment, the fans were turned off, the logger data was transferred to a computer as an Excel file, and the logger was switched off immediately so that it could not collect further data. It is possible for the data recorder to measure after the data is collected, and that measurement would be included in the data for the following experiment and would need to be removed manually. The eggplant was removed from the dryer and weighed after turning off all equipment.

3.5. Attaching the net on the absorber

The roughened absorber plates were made by attaching aluminium wire with a 1 mm square cross-section and a 13 mm gap between the net and the text thread. The net was cut according to the absorber plate dimensions and carefully placed transversely to the streamwise direction on the top and bottom of the absorber in the same direction. Clips and adhesive were used to secure the net to the absorber plate's edges, ensuring it remained taut and flat. Then, calculate the inlet and outlet temperatures, heat flux, and absorber efficiency, and analyse the temperature data to evaluate heat transfer in the solar dryer.

Figure 4. This figure shows the absorber with net attaching on it. The nets and absorber were painted black before being covered with glass.

3.6. The verification of a constant drying rate

As a result of only measuring the weight of the eggplant before and after drying, it was necessary to confirm that the assumption of a linear decrease in weight was a valid estimate. The linearity of weight loss over time was confirmed through three distinct flows. The drying tests were conducted in the same manner as described previously; except this time the weight of a designated shelf was measured hourly. A linear fit was applied along with an R^2 value to the measured weight against time to verify the weight loss's linearity.

3.7. The verification of even drying

The progress of the eggplant's drying was measured to test the assumption of even drying in the solar dryer. Eggplant samples were placed in removable trays, shown in Fig. 5, and their weight was recorded every hour during the drying process. The expectation was that all samples would experience similar drying rates and weight losses during drying time, regardless of their location in the tray.

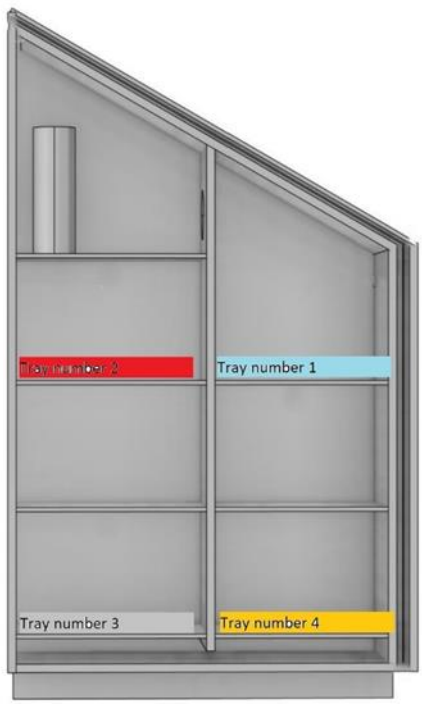

Figure 5. *This photo shows the arrangement of various removable trays that were utilized to take hourly measurements.*

3.8. Make the holes

To increase airflow and drying, holes could be drilled into the chamber wall of the solar dryer shown in Fig. 1. It is hypothesized that incorporating additional holes in chosen places would increase air circulation also to disturb the flow and thus drying effectiveness. This hypothesis was tested by drilling holes in both the middle and bottom of a solar dryer chamber wall and comparing the effectiveness of this configuration to a standard configuration without holes.

Figure 6. The picture shows the wall of the dryer chamber with drilled holes.

3.9. Open air drying

In order to compare open-air drying with the dryer, two experiments were conducted: one in the shade and one in direct sunlight. In this experiment, eggplant was prepared in the same manner and dried at the same time as in the experiments with the dryer. During the experiment, the weight of the

product was measured before and after the experiment to determine the rate at which it dried.

3.10. Calculations

In order to save time and prevent human errors, all experiments were handled using the same procedure. Excel's Visual Basic for Applications was used to develop the script that sorted the data into separate tabs for each component and generated corresponding charts. Unreasonably large values were obtained when the division was near zero, so some filtering was required for ratio and efficiency measurements. This was done to prevent large values from affecting the daily average efficiency.

3.10.1. Absorber efficiency

A viable method for determining the absorber's efficiency is to divide the solar flux available by the heat absorbed by the air. A solar flux calculation was made by multiplying the measured irradiance I by the absorber's surface area A, which is 0.5 m², and the heat absorbed by the air was determined by using Eq. 6.

In order to calculate the efficiency of the absorber, Eq. 15 is used.

$$\eta = \frac{V_{air} A_{cross} \rho_{air} C_p \Delta T}{IA} \qquad Eq. 15$$

4. Results

4.1. Hourly weight measurement

The graph shows the drying rate. As the graph shows, the drying rate is constant throughout the time. The results of the hourly weight measurement used to confirm that the drying rate is constant closely followed a linear

pattern. The fact that the R^2 values of all three linear fits are higher than 0.99 provides strong evidence supporting the hypothesis of a constant drying rate.

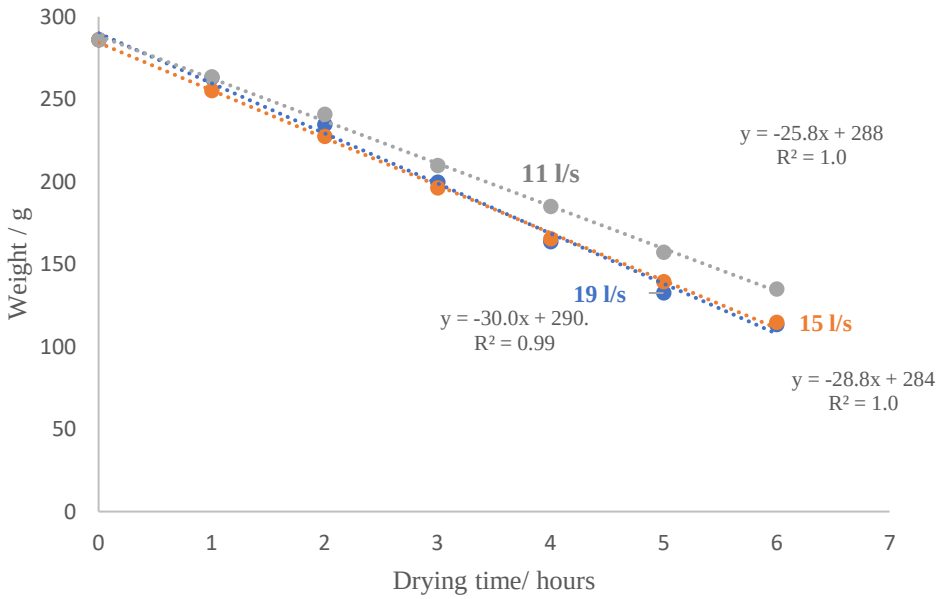

Figure 7. A graph showing the hourly weight of eggplant over time for three different experiments, one with a flow of 11 l/s (gray), one with a flow of 15 l/s (orange), and one with a flow of 19 l/s (blue). A linear fit of each experiment is determined by the R^2 -value.

4.2. Drying characteristic of eggplant

An evaluation of the outcomes of drying eggplant slices is shown here. Fig. 8, 9 and 10 depict the variation in eggplant weight as a function of drying duration at various trays. Each figure corresponds to an individual flow. It can be seen from these data that, at a constant time, the weight loss is almost uniform across different trays. Furthermore, as can be seen from the Fig. 8, 9 and 10 the higher flow is associated with higher drying rate.

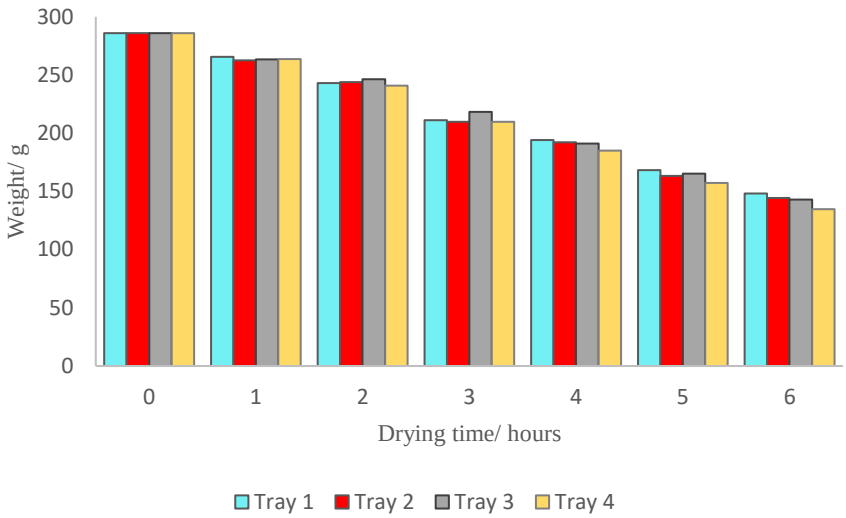

Figure 8. This graph illustrates the weight of eggplant in various trays within a chamber over time, at a flow of 11 l/s. The color of each column indicates the location of the tray.

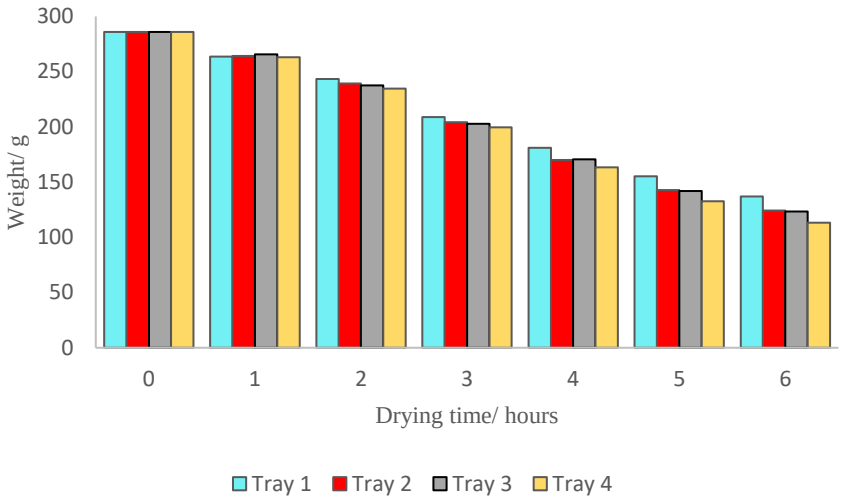

Figure 9. This graph illustrates the weight of eggplant in various trays within a chamber over time, at a flow of 15 l/s. The color of each column indicates the location of the tray.

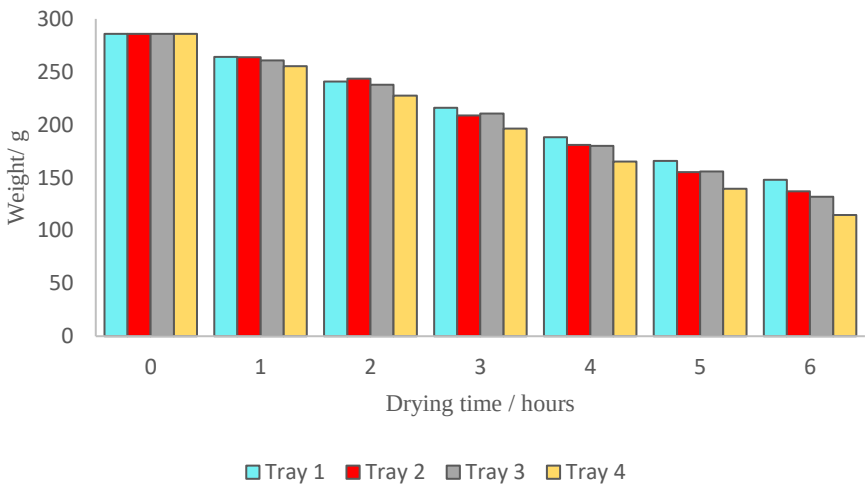

Figure 10. This graph illustrates the weight of eggplant in various trays within a chamber over time, at a flow of 19 l/s. The color of each column indicates the location of the tray.

4.3. Weight Measurement with and without holes

Experiments were conducted with 2 kilograms of eggplant, dried for 6 hours with and without holes in the drying chamber's wall with the same flow. Although the difference between with and without holes is small, there is evidence that without holes is preferable. The conditions of two experiments are given in Table 1.

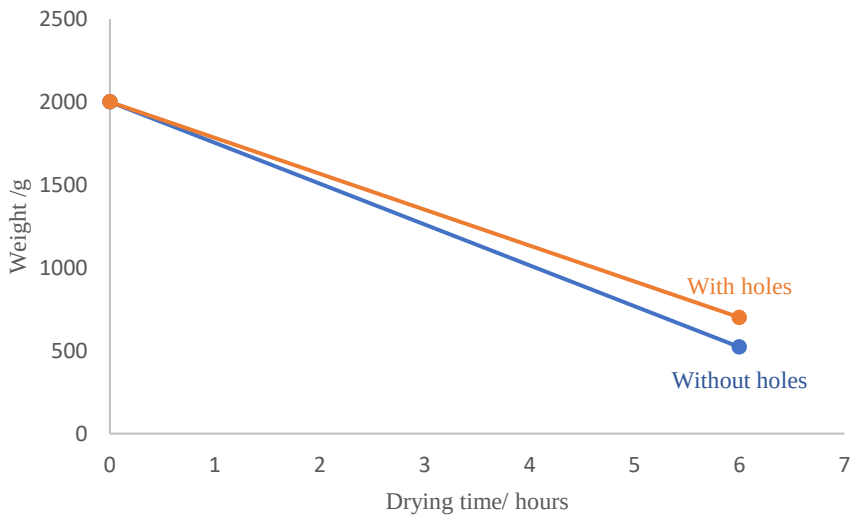

Figure 11. Eggplant weight over time for two separate experiments, one without holes (blue) and one with holes in the chamber's wall (orange) in a flow of 19 l/s.

Table 1. The table provides information regarding two separate days on which two experiments were conducted.

	Flow / (l/s)	Drying rate / (g/h/m²)	Average Ambient Temperature / (°C)	Average Solar Irradiation / (W/m²)	Average Chamber Temperature / (°C)
Without holes	19	320	31	521	34
With holes	19	283	31	496	34

4.4. Drying Rate

The graph indicates an increase in the drying rate as the chamber temperature increases. Changes in absorber surface affect both temperature and drying rate. In accordance with the obtained data, the chamber temperature was lower when the net was placed on the absorber as compared to the condition without any modification. The differences in temperature between the two conditions can be attributed to differences in average solar radiation during these experiments. The conditions of experiments without net and with net on the absorber are given in Table 2 and Table 3.

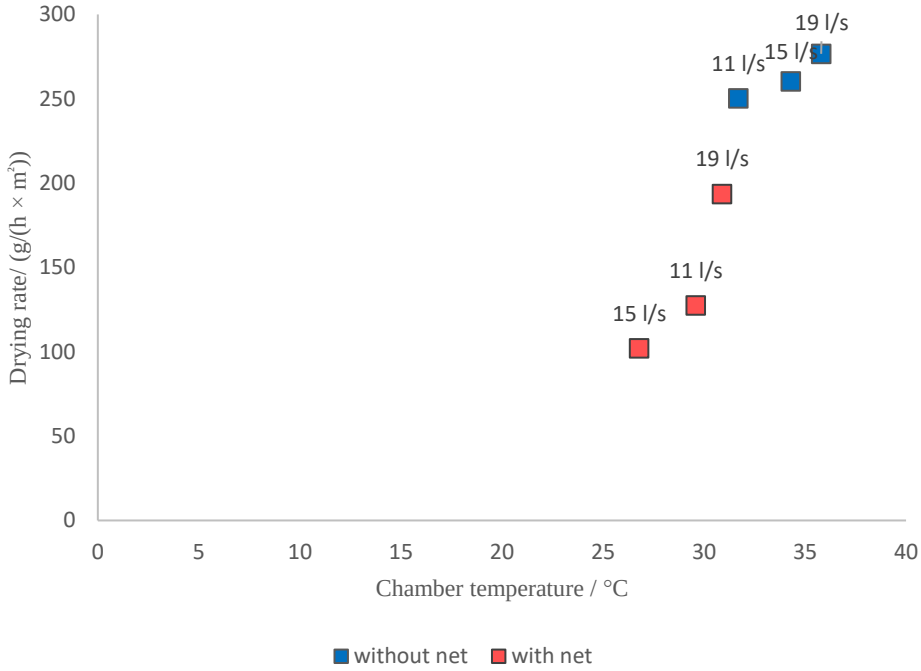

Figure 12. It shows drying rate as a function of chamber temperature and different flow is indicated with text. The blue square dots indicate cases without a net, while the red one indicate cases with a net. The number displayed above each square dot indicates the flow of each experiment.

Table 2. This table provides information regarding three separate days in which three experiments were conducted without net on the absorber.

Flow / (l/s)	**Drying Rate / (g/h/m^2)**	**Average Ambient Temperature / (°C)**	**Average Solar Irradiation / (W/m²)**	**Average temperature Before Absorber / (°C)**	**Average temperature After Absorber / (°C)**
19	276	32	514	33	45
15	260	30	671	32	50
11	251	29	581	31	51

Table 3. This table provides information regarding three separate days in which three experiments were conducted with net on the absorber.

Flow / (l/s)	**Drying Rate / (g/h/m^2)**	**Average Ambient Temperature / (°C)**	**Average Solar Irradiation / (W/m²)**	**Average temperature Before Absorber / (°C)**	**Average temperature After Absorber / (°C)**
19	193	27	328	28	34
15	102	24	186	25	30
11	127	28	385	29	39

Without changing the absorber, a higher flow results in a faster drying rate for the dryer. The dryer's maximum drying rate was measured using a flow of 19 l/s, yielding a drying rate of 276 g/ (h ×m²). The Fig. 13 shows the drying rate in the direct sun is lower than the drying rate with the lowest flow in the dryer in base case. Even at the lowest flow 11 l/s, drying is faster than in the air under direct sunlight. In open-air drying experiments, there is no predetermined airflow.

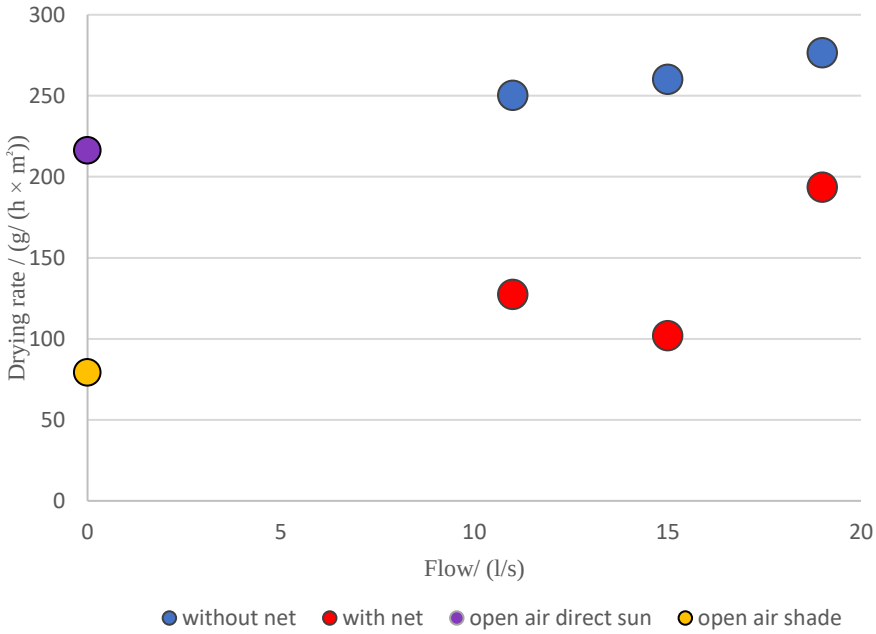

Figure 13. The drying rate is plotted over flow. The blue dots indicate cases without a net, while the red dots indicate cases with a net. Yellow and purple dot indicate open sun drying in the shade and in direct sunlight, respectively.

4.5. Heat exchanger

Heat exchanger efficiency was calculated by Eq. 12. As the flow increases, the efficiency of the heat exchanger decreases. Average efficiency reached 78 % at 11 l/s, the highest measured value. A linear decline in efficiency occurs from flow 11 l/s to 15 l/s, followed by a gradual decline from 11l/s to 19 l/s.

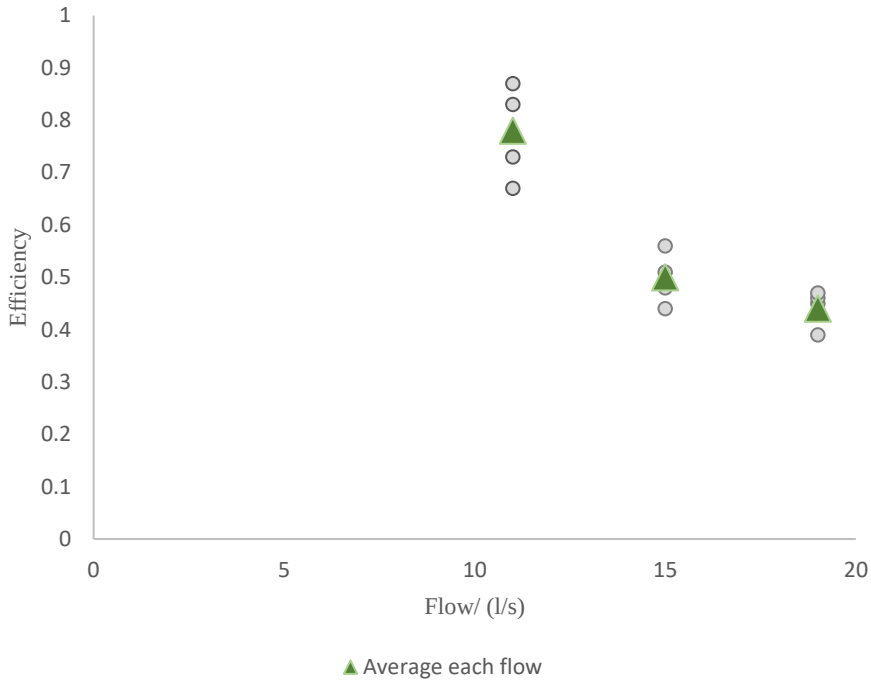

Figure 14. Heat exchanger efficiency plotted over flow. In each flow, every dot represents the result of one experiment, and the triangle represents the average efficiency of different experiments.

4.6. Absorber

Absorber efficiency was calculated by Eq. 13. The results indicate that increasing the flow has little impact on the absorber's efficiency. Cloud cover, atmospheric conditions, or shading may have contributed to the disparity in average solar radiation between the experiments with and without the net. Experiments without a net and with a net on the absorber are described in Tables 2 and 3, respectively. Solar energy availability can be affected by these factors, which can affect the absorber's overall performance.

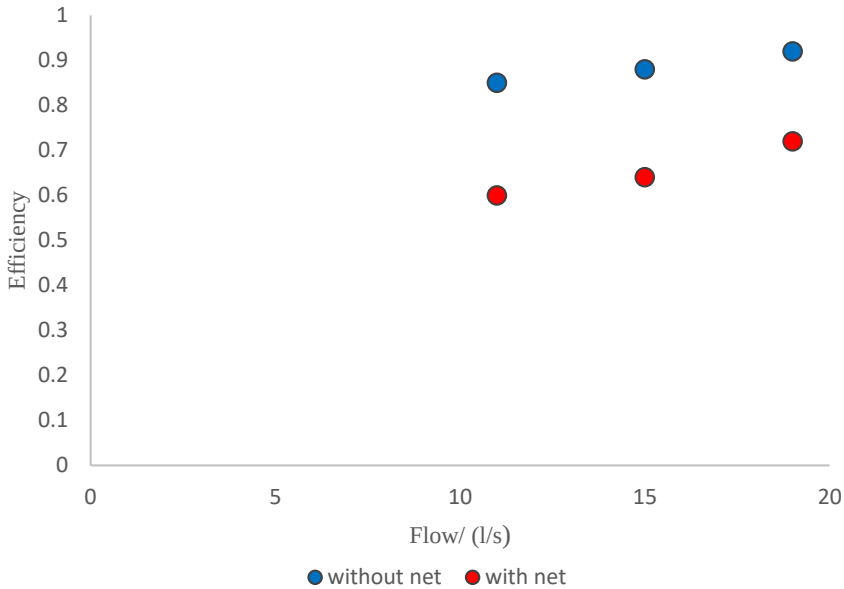

Figure 15. The average efficiency of the absorber plotted over flow. A blue dot indicates an absorber without a net, whereas a red dot indicates an absorber with a net.

4.7. Drying chamber

A drying chamber temperature was measured for three different flows with and without nets on the absorber in Fig. 16. For highest flow, the average chamber temperature reaches almost 36 for the base case.

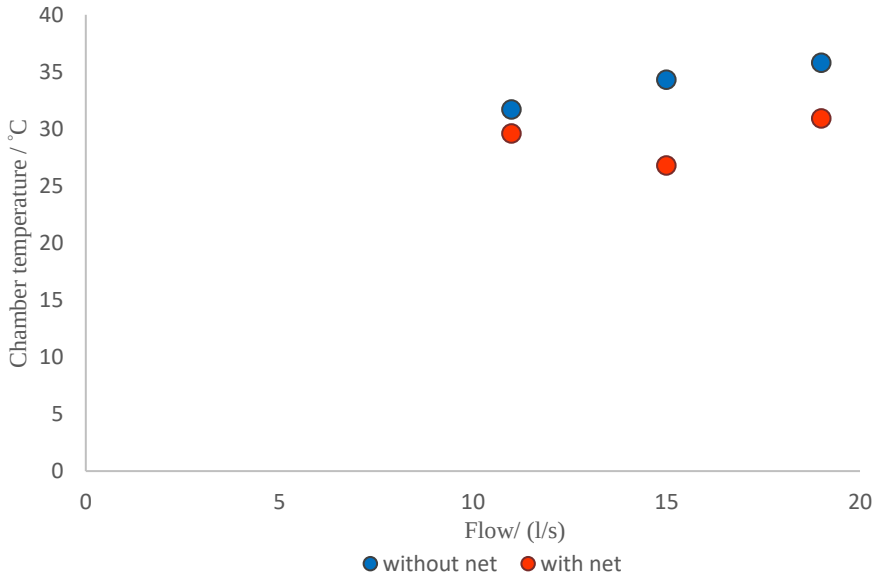

Figure 16. The average chamber temperature was plotted against different flows. The blue dots indicate cases without a net, while the red dots indicate cases with a net.

4.8. Individual analysis

4.8.1. Absorber

It is difficult to compare the efficiencies of absorbers due to the variability of solar radiation, particularly early in the day. In order to obtain a more precise and consistent comparison of absorber efficiency, excessive variability was eliminated. Analyzing stable periods reveals information regarding the relative performance of absorbers with and without a net. The average efficiency was calculated after 13:00 pm.

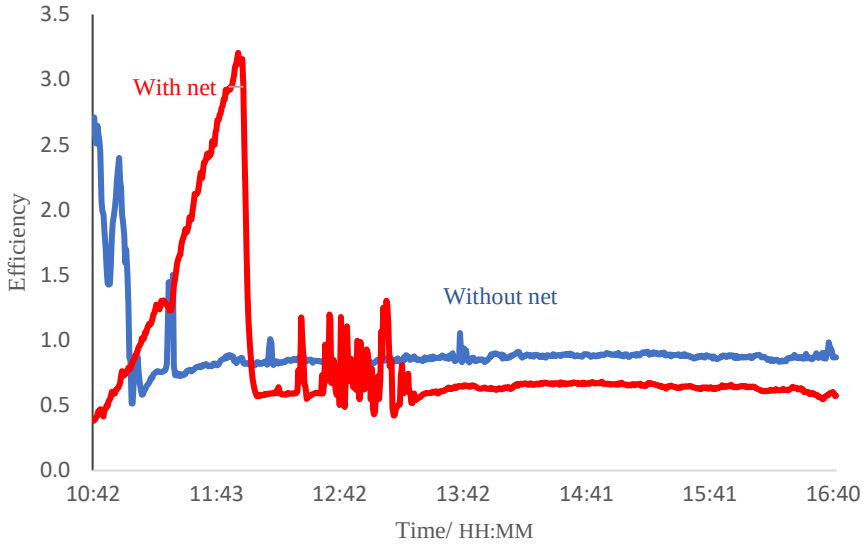

Figure 17. Shows the absorber efficiencies measured during two days with a flow rate of 15 l/s. The blue line represents the efficiency of the absorber without a net, while the red line represents the efficiency of the absorber with a net.

Based on the temporal analysis of the radiation graph, distinct patterns were observed before and after 13:00 PM. The graph showed significant fluctuations in radiation levels before 13:00 PM, indicating an environment that could impact the efficiency of absorption. In contrast, radiation levels decreased post-midday without any notable fluctuations, suggesting a more stable and predictable radiation environment.

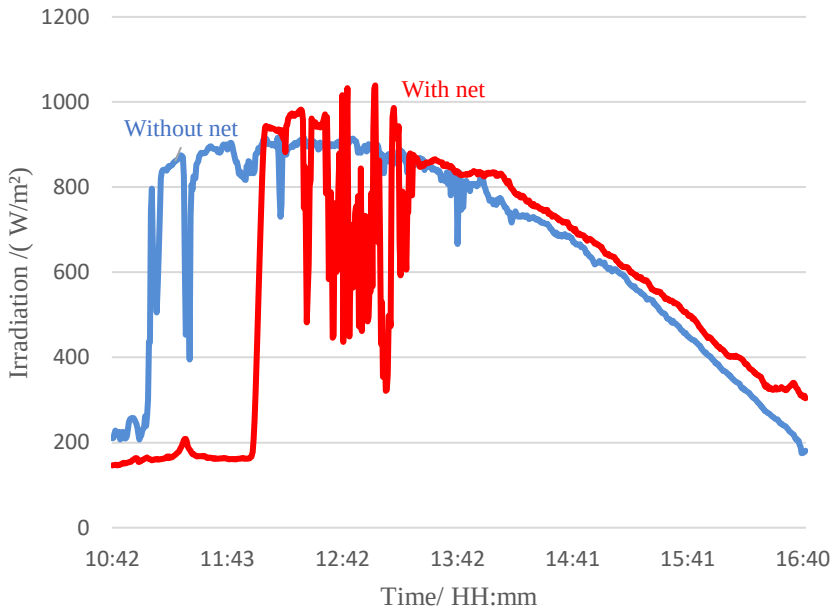

Figure 18. The data displayed the radiation from the same experiments as Figure 17 with a 15 l/s flow rate. The blue line shows the experiment without a net on the absorber, while the red line shows the experiment with a net.

4.8.2. Heat exchanger

It took some time for the heat exchanger to produce consistent results. The gray line represents the ratio between the temperature differences on the cold and hot sides. There were some days when the ratio was below 1.0 and some days when it was above 1.0, but nothing was consistent enough to suggest leaking. During the morning, the temperature ratio fluctuated greatly. After midday, consistency returned to the outcomes.

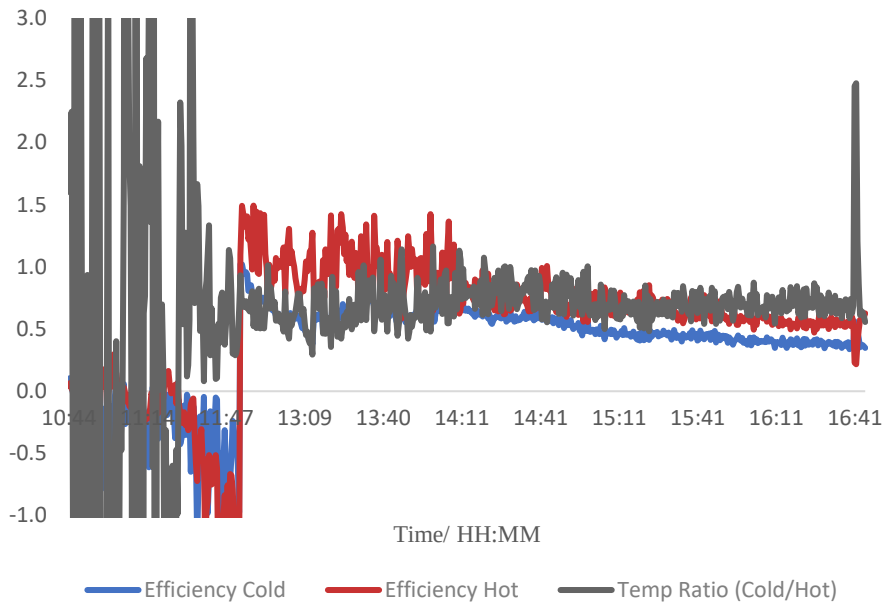

Figure 19. depicts the heat exchanger efficiencies and temperature difference ratio determined on April 25, 2023, during an experiment utilizing 15 l/s. The blue line indicates the efficiency measured on the cold side, while the red line indicates the efficiency measured on the hot side. The gray line represents the ratio of the temperature difference observed on the cold side to the temperature difference observed on the hot side.

4.8.3. Drying chamber

A steady temperature rise is observed within the drying chamber throughout the morning, accompanied by an equally noticeable rise in the entering air temperature. While the chamber temperature rises between 12:00 and 14:00, the intake air remains relatively constant at roughly 47 °C. We see a significant drop in incoming air temperature after 14:00; however, the chamber temperature holds steady between 33 °C and 36 °C and experiences a prolonged drop towards the end.

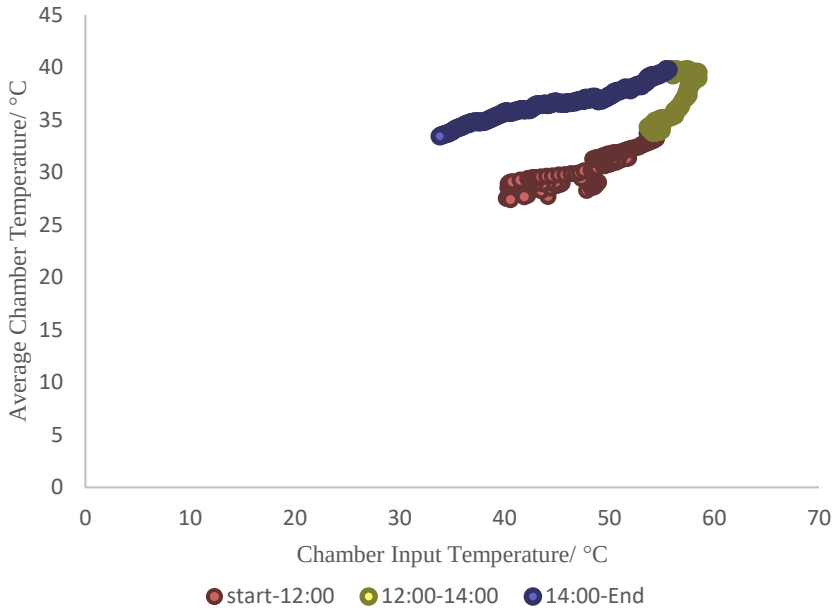

Figure 20. Plot of the temperature of the drying chamber versus the temperature of the air exiting the absorber. In the following graph, the red dots represent measurements taken before 12:00, the yellow dots represent measurements taken between 12:00 and 14:00, and the blue dots represent measurements taken after 14:00. The experiment was conducted on 08/04/2023 with a flow of 15 l/s.

Comparing the temperature inside the dryer with that outside shows a similar pattern as found in Fig. 20; however, a roughly constant trend is observed instead of a slight decline in the evening. As of around noon, the incoming air temperature will gradually approach the chamber temperature until later in the evening, when it becomes cooler, thereby cooling the dryer.

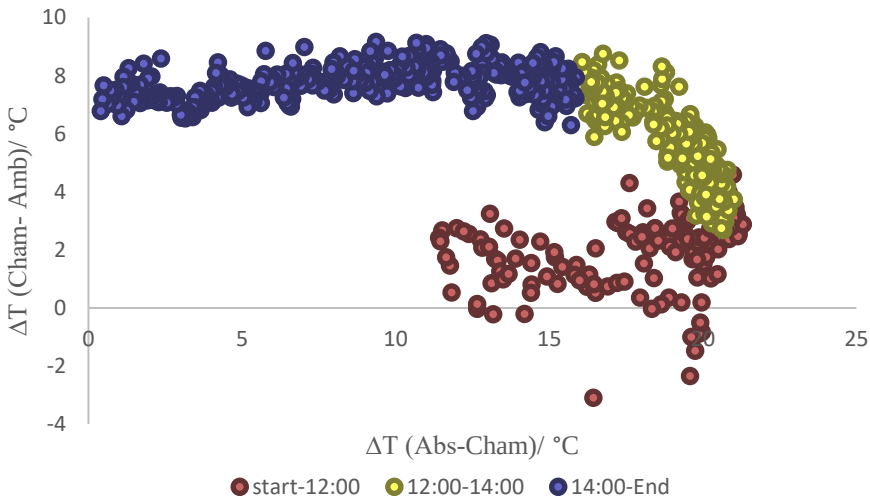

Figure 21. The relative temperature of the drying chamber. The Y-axis represents the temperature difference between the chamber and the surrounding air, while the X-axis represents the temperature difference between air after passing through the absorber and the chamber. These results also come from the same experiment as figure 20.

5. Discussion

This study aimed to determine how flow disturbance affects solar dryer performance. It was proposed that roughness be introduced to disrupt the flow and enhance heat transfer within the system. As a result of the collected data, each component of the solar dryer was analyzed under different absorber conditions.

Although artificial roughness can enhance heat transfer and drying performance, external factors may affect its effectiveness. Variations in operating conditions, such as air velocity, ambient temperature, and relative humidity, can impact the efficiency of the roughness in disrupting the flow and promoting convective heat transfer. In the experiments, weather conditions made it difficult to directly compare the solar dryer performance with and without the net.

5.1. Drying rate

The drying rate is a crucial parameter in the performance evaluation of a drying system, as it determines the efficiency and effectiveness of the drying process. In this study, the drying rate was examined to assess the impact of changing air flow and modifying the absorber surface on the drying performance.

It was observed that higher air flow rates resulted in faster drying times, indicating an accelerated moisture removal from the samples. Nevertheless, further improvements are challenging due to the external fan in the current system. It's important to note that if there isn't a tunnel to measure flow, air will move through the dryer with less resistance, which could lead to higher flows. Both the dryer's internal and external fans should be turned up to high if it is only going to be used for drying in the future and not for experiments.

Maximizing heat absorption within the solar dryer can accelerate the drying process. Depending on the absorber size and temperature rise, a system with a higher drying rate within the range of achievable flows may have different results. It is a point at which enough air can flow without affecting the temperature too much. By improving the flow in the solar dryer, materials can be dried faster and more efficiently. It's important to consider this factor.

Increasing airflow typically requires more energy, mainly when powered fans are employed. This can increase the solar dryer's energy consumption and operational costs. It is important to consider limitations such as availability, cost, and energy consumption when redesigning the solar dryer to increase airflow. The use of locally available resources and a larger solar absorber could provide a cost-effective approach in rural Bhutan. By capturing more solar radiation, the dryer can generate more heat.

Air humidity plays a crucial function in the drying process. Increased air humidity can inhibit the evaporation of moisture, resulting in a delayed drying rate. Seasonal factors, such as temperature and humidity, can influence the choice of flow. Drying without increasing the temperature on a day with high humidity is impossible. Therefore, the results of a similar study conducted during a hot summer or cold winter may differ from those obtained here.

5.2. Heat exchanger

In this study, When the flow rate is increased, the air moves more rapidly through the heat exchanger. As a result, the contact time between the air and

the heat exchanger surfaces decreases. This reduced contact time limits the opportunity for effective heat transfer between the air and the heat exchanger, thereby lowering the overall efficiency of the heat exchange process. The results showed that Heat exchanger efficiency increased with both reduced flow and increased contact time while heat flux between the sides remained essentially constant. Because of this, the larger temperature difference due to the improved performance of the absorber is mitigated to some extent by the decrease in efficiency.

5.3. Drying chamber

In order to analyze the drying rate and its relationship with heat transfer, it is important to consider the temperature within the drying chamber. The temperature of a drying chamber plays a significant role in determining the efficiency of heat transfer and the drying process in general.

The dryer interior temperature during the 15 l/s flow test is shown in Fig. 20. The data reveals that temperatures rise steadily throughout the morning, remain relatively consistent throughout the noon, and then begin to fall gradually by the afternoon. The difficulty is that the temperature stays below 60 °C, which is usually accepted as best for drying since it helps eliminate microorganisms. In the base condition, the chamber climbed barely above 40 °C even at the highest flow. It supports the idea that a larger absorber would significantly enhance the dryer's design. However, it is essential to consider the system's overall design, insulation, and energy supply to maintain optimal drying conditions while avoiding overheating and material damage.

5.4. Absorber

In this report, the impact of creating artificial roughness on the absorber surface of a solar dryer was investigated. A net is used in this study as an artificial roughness on the absorber surface in order to enhance heat transfer and improve drying efficiency. The results demonstrate that increasing the flow has a minimal effect on efficiency. Fig. 15 indicates that although efficiency may increase slightly with higher flow, the difference is insignificant. It is important to note that the impact of roughness on the absorber surface may vary depending on the specific design and operating conditions of the solar dryer. Factors such as air velocity, ambient temperature, and relative humidity can influence the effectiveness of the roughness in enhancing heat transfer.

These findings contribute to a deeper understanding of absorber behavior and provide valuable insights for designing more efficient absorber systems. Therefore, optimizing other factors, such as surface area or material properties, may be more effective in enhancing absorber performance.

5.5. Weather conditions

The changing weather conditions during the experiment had a significant impact on the results, which should be noted. The solar drying process heavily relies on sunlight and ambient temperature, which can fluctuate considerably due to weather changes. Drying rate, moisture content, and overall performance were affected by these fluctuations. The results in Table 2 indicate that drying rates are higher on days with clear skis and ample sunlight, and the intense solar radiation provided optimal conditions for heat transfer. As a result, the drying time was shortened.

However, days with overcast skies, rain, or low solar radiation posed challenges to the solar drying process. Due to the reduced availability of sunlight, the drying process was slower. Based on the information in Table 3, inadequate solar radiation restricted the amount of heat input, resulting in an extended drying time.

6. Conclusion

The study showed that increasing the airflow reduced the drying time of the samples. The products lost moisture faster when the airflow was higher, leading to shorter drying times. As a result, higher airflow helps remove moisture more efficiently and speeds up drying. It also showed the homogeneous drying process within the chamber.

The experiment where holes were drilled into the chamber's walls showed that the chamber without holes was somewhat more effective. However, several factors could have affected the accuracy of these measurements, such as the thickness of the product or the amount of sunlight and wind.

It was observed that higher flow rates resulted in lower heat exchanger efficiencies, which represents an inverse relationship between these variables. In the experiments, heat exchanger efficiency averaged 78% at the lowest

flow and 44% at the maximum. Heat exchangers may be more useful in dryer designs that generate higher internal temperatures, so it is important to carefully consider the experiment's specific conditions and the system's design. Modifying the heat exchanger design or optimizing the flow may be necessary to achieve the desired efficiency and performance. Still, it is debatable whether the additional costs and effort are worth.

It was determined that flow rate has a minimal impact on absorber efficiency in this study. In this study, a solar dryer was evaluated while using an artificially roughened absorber. The drying rate, temperature after absorber, and chamber temperature were all shown to be lowered when a net was added as roughness to the absorber. However, the variability in weather conditions hindered a comprehensive comparison between solar dryer with and without a net on the absorber.

Nonetheless, because of weather fluctuations, it was not able to replicate the studies under the same radiation or ambient temperature. Therefore, it is impossible to compare the performance of solar dryers with and without a net on the absorber based on these measurements.

In conclusion, a larger absorber, a larger fan if price and availability allow, and enhanced insulation would significantly improve the dryer's design.

7. Limitation and Future work

Some limitations were encountered during our experiments with the solar dryer in Bhutan that may have influenced the results and validity of our findings. Finding the necessary equipment and materials for an experiment in some remote or underdeveloped areas can take time and effort. This can limit the scope of the experiment. For this study, limited resources and equipment posed a challenge in conducting all the planned experiments.

The weather can affect how well solar dryer’s work. Bhutan's unpredictable and changing weather conditions presented an additional challenge to our experiments. The temperature, humidity, and solar radiation variability affected the drying process and made it difficult to maintain consistent and controlled experimental conditions. As a result, these weather variations may impact the outcomes, which could affect the validity and reproducibility of our findings. Research in the future should examine strategies for mitigating the effects of weather variability, such as choosing specific experimental periods.

Future experiments could be conducted by varying the size or shape of the net openings or by orienting them differently on the absorber surface, such as

vertically, at an angle from the flow, or by spinning the absorber. Various net materials and configurations can be tried to determine what is the most suitable option for the absorber. Investigate different designs or patterns for the net that can enhance its effectiveness.

Throughout these tests, a constant voltage was applied to the internal fan. By varying the fan airflow inside the chamber, it may be possible to determine whether drying results can be improved and by how much. There is a potential for increased drying rates with less energy consumption, which motivates further study.

Solar dryer heat exchangers facilitate efficient heat transfer and maximize drying processes, especially in systems with high internal temperatures. Throughout this report, a heat exchanger is constructed from a flat aluminum sheet. With further optimization, the performance of the heat exchanger could change if a turbulent flow is reached. A heat exchanger could achieve this by exploring advanced heat transfer surfaces, such as finned or corrugated surfaces, to increase the area available for heat transfer. Surfaces such as these can enhance convective heat transfer and improve drying efficiency.

References

Akpinar, E.K., Bicer, Y. and Yildiz, C., 2003. Thin layer drying of red pepper. *Journal of food engineering*, *59*(1), pp.99-104.

Alam, T. and Kim, M.H., 2017. A critical review on artificial roughness provided in rectangular solar air heater duct. *Renewable and Sustainable Energy Reviews*, *69*, pp.387-400.

Alamu, O.J., Nwaokocha, C.N. and Adunola, O., 2010. Design and construction of a domestic passive solar food dryer. *Leonardo Journal of Sciences*, (16), pp.71-82.

Bala, B.K. and Woods, J.L., 1994. Simulation of the indirect natural convection solar drying of rough rice. *Solar Energy*, *53*(3), pp.259-266.

Bechoff, A., Dufour, D., Dhuique-Mayer, C., Marouzé, C., Reynes, M. and Westby, A., 2009. Effect of hot air, solar and sun drying treatments on provitamin A retention in orange-fleshed sweetpotato. *Journal of Food Engineering*, *92*(2), pp.164-171.

Bergman, T.L., Bergman, T.L., Incropera, F.P., Dewitt, D.P. and Lavine, A.S., 2011. *Fundamentals of heat and mass transfer*. John Wiley & Sons.

Brooker, D.B., Bakker-Arkema, F.W. and Hall, C.W., 1992. *Drying and storage of grains and oilseeds*. Springer Science & Business Media.

Çengel, Y.A. and Ghajar, A.J., 2002. Heat Conduction Equation. *Heat Transfer A Practical Approach, 2nd ed. McGraw-Hill Higher Education*, pp.61-126.

Chhogyel, N. and Kumar, L., 2018. Climate change and potential impacts on agriculture in Bhutan: a discussion of pertinent issues. **Agriculture & food security**, **7**(1), pp.1-13.

Climate Research Unit of University of East Anglia. 2020. Climate Change Knowledge Portal. Accessed 08 23, 22. https://climateknowledgeportal.worldbank.org/country/bhutan/climate-data-historical.

Chua, K.J., Chou, S.K., Hawlader, M.N.A., Mujumdar, A.S. and Ho, J.C., 2002. Modelling the moisture and temperature distribution within an agricultural product undergoing time-varying drying schemes.

Davidsson, H., Olsson, J., Phinney, R., Bernardo, R., Otte, P. and Tivana, L., 2017. Towards a homogenous drying rate using a solar fruit dryer. In *ISES, International solar energy society, Solar World Congress 29 Oct–02 Nov 2017, Abu Dhabi, UAE*.

Davidsson, Henrik. 2021. "Canvas." Solar collector physics. Accessed 08 31, 2022. https://canvas.education.lu.se/courses/14485/files/1675057?module_item_id=407937.

Doymaz, İ., 2005. Drying behaviour of green beans. *Journal of food Engineering*, *69*(2), pp.161-165.

El-Sebaii, A.A. and Shalaby, S.M., 2012. Solar drying of agricultural products: A review. *Renewable and Sustainable Energy Reviews*, *16*(1), pp.37-43.

Ertekin, C. and Yaldiz, O.S.M.A.N., 2004. Drying of eggplant and selection of a suitable thin layer drying model. *Journal of food engineering*, *63*(3), pp.349-359.

Frame, B. (2005) 'Bhutan: A review of its approach to sustainable development', **Development in Practice**, 15(2), pp. 216–221.

Gallali, G; Garg, H.P; and Prakash, J. 2000. Solar drying versus open sun drying, A framework for financial evaluation, Solar Energy, vol. 80, pp. 1568-1579.

Ghatrehsamani, S.H., Dadashzadeh, M. and Zomorodian, A., 2012. Kinetics of apricot thin layer drying in a mixed and indirect mode solar dryer. *International Journal of Agriculture Sciences*, *4*(6), p.262.

Hamdi, I., Kooli, S., Elkhadraoui, A., Azaizia, Z., Abdelhamid, F. and Guizani, A., 2018. Experimental study and numerical modeling for drying grapes under solar greenhouse. *Renewable Energy*, *127*, pp.936-946.

Hale, D.V., Hoover, M.J. and ONeill, M.J., 1971. *Phase change materials handbook* (No. NASA-CR-61363).

Hesselgreaves, J.E., Law, R. and Reay, D., 2016. *Compact heat exchangers: selection, design and operation*. Butterworth-Heinemann.

Jain, D. and Tiwari, G.N., 2004. Effect of greenhouse on crop drying under natural and forced convection I: Evaluation of convective mass transfer coefficient. *Energy conversion and Management*, *45*(5), pp.765-783.

JNEC. n.d. About the Collage. Accessed 10 2022. https://www.jnec.edu.bt/en/ourcollege/.

Johansson, P. and Svensson, A., 2007. *Metoder för mätning av luftflöden i ventilationsinstallationer*. Byggforskningsrådet.

Kumar, M., Sansaniwal, S.K. and Khatak, P., 2016. Progress in solar dryers for drying various commodities. *Renewable and Sustainable Energy Reviews*, *55*, pp.346-360.

Kumar, P. and Singh, D., 2020. Advanced technologies and performance investigations of solar dryers: A review. *Renewable Energy Focus*, *35*, pp.148-158

Madhlopa, A., Jones, S.A. and Saka, J.K., 2002. A solar air heater with composite–absorber systems for food dehydration. *Renewable energy*, *27*(1), pp.27-37.

Mercer, D.G., 2014. *An introduction to the dehydration and drying of fruits and vegetables*. Donald G. Mercer.

Mujumdar, A.S., 2006. Principles, classification, and selection of dryers. *Handbook of industrial drying*, *3*, pp.3-32.

Murthy, M.R., 2009. A review of new technologies, models and experimental investigations of solar driers. *Renewable and Sustainable Energy Reviews*, *13*(4), pp.835-844.

Mustayen, A.G.M.B., Mekhilef, S. and Saidur, R., 2014. Performance study of different solar dryers: A review. *Renewable and Sustainable Energy Reviews*, *34*, pp.463-470.

Panchariya, P.C., Popovic, D. and Sharma, A.L., 2002. Thin-layer modelling of black tea drying process. *Journal of food engineering*, *52*(4), pp.349-357.

Prasad, B.N. and Saini, J.S., 1988. Effect of artificial roughness on heat transfer and friction factor in a solar air heater. *Solar energy*, *41*(6), pp.555-560.

Rahman, M.S. and Perera, C.O., 2007. Drying and food preservation. In *Handbook of food preservation* (pp. 421-450). CRC Press.

Rosengren, A. (2017). *Inläggning, gravning, syrning och konservering* (Rapport 8 del 1). Swedish Food Agency https://www.livsmedelsverket.se/globalassets/publikationsdatabas/rapporter/2017/rikshanteringsrapport_ inlaggninggravningsyrningochkonserveringlivsmedelsverket-rapport82017del1.pdf

Sarker, A., Islam, M.N. and Shaheb, M.R., 2012. A study on the drying behaviour of a local variety (Lalpakri) of potato (Solanum tuberosum L.). *Bangladesh Journal of Agricultural Research*, *37*(3), pp.505-514.

Shah, R.K., London, A.L., White, F.M., 1980. Laminar Flow Forced Convection in Ducts. Journal of Fluids Engineering 102, 256–257. https://doi.org/10.1115/1.3240677

Sharma, A., Chen, C.R. and Lan, N.V., 2009. Solar-energy drying systems: A review. *Renewable and sustainable energy reviews*, *13*(6-7), pp.1185-1210.

The Engineering Toolbox. 2003. *Emissivity Coefficients common Products. Accessed 08 26, 2022.* *https://www.engineeringtoolbox.com/emissivity-coefficientsd_447.htm*

The Engineering Toolbox. 2003. *Air - Density, Specific Weight and Thermal Expansion Coefficient vs. Temperature and Pressure. Accessed 08 31, 2022*.

Air - specific heat vs. temperature at constant pressure , Engineering ToolBox. Available at: https://www.engineeringtoolbox.com/air-specific-heat-capacity-d_705.html (Accessed: 20 June 2023).

The World Bank. 2022. *The World Bank. Accessed 09 01, 2022*

Toğrul, İ.T. and Pehlivan, D., 2004. Modelling of thin layer drying kinetics of some fruits under open-air sun drying process. *Journal of food Engineering*, *65*(3), pp.413-425.

Tomar, V., Tiwari, G. and Norton, B., 2017. Solar dryers for tropical food preservation: Thermophysics of crops, systems and components. *Solar Energy*, *154*, pp.2-13.

Toolbox, E., 2003. Water—Density, Specific Weight and Thermal Expansion Coefficient. *New Haven, CT, USA: The Engineering ToolBox*.

Tiwari, A., 2016. A review on solar drying of agricultural produce. *Journal of Food Processing & Technology*, *7*(9), pp.1-12.

Udomkun, P. *et al.* (2020) *Review of solar dryers for agricultural products in Asia and Africa: An innovation landscape approach*, *Research@WUR*. Available at: https://research.wur.nl/en/publications/review-of-solar-dryers-for-agricultural-products-in-asia-and-afri (Accessed: 15 May 2023).

Waewsak, J., Chindaruksa, S. and Punlek, C., 2006. A mathematical modeling study of hot air drying for some agricultural products. *Science & Technology Asia*, pp.14-20.

Wang, L. and Sundén, B. (2006) 'Experimental investigation of local heat transfer in a square duct with various-shaped ribs', *Heat and Mass Transfer*, 43(8). doi:10.1007/s00231-006-0190-y.

Whalley, J., 2004. Telecommunications in the land of the Thunder Dragon: recent developments in Bhutan. **Telecommunications Policy**, **28**(11), pp.785-800.

WFP. 2020. "World Food Programme." WFP's support to Nutrition in Bhutan. Accessed 08 16, 2022. https://reliefweb.int/report/bhutan/wfp-s-support-nutrition-bhutan.

World Bank, 2005. **World development indicators 2005**. The World Bank.